

FIG. 3. Calculated $\ln(C_2/C_1)$ vs $\ln \epsilon$. The straight line is a linear fit.

simple Hamiltonian, Δ can indeed deviate greatly from the mean-field value. Therefore, a measured Δ (even if it is close to tricritical exponent) that disagrees with the mean-field value does not constitute a conclusive verification that the nematic-isotropic transition is not an ordinary critical point. It only says that the mean-field approximation is not good enough in describing this transition. Of course, the possibility of a tri-

critical point is not precluded. But this needs other evidence. In this regard, theoretical investigations along the line presented here with use of a more realistic Hamiltonian is most desired. In fact, preliminary results are rather encouraging and will be reported elsewhere.

We thank Glenn H. Brown, William L. McMillan, and Chia-Wei Woo for helpful discussions and various people at Northwestern University for their kind hospitality during the author's stay. This work is supported in part by the National Science Foundation through Grant No. DMR 76-18375.

^(a)Permanent and correspondence address.

¹P. H. Keyes and J. R. Shane, *Phys. Rev. Lett.* **42**, 722 (1979).

²P. G. de Gennes, *Phys. Lett.* **30A**, 454 (1969), and *Mol. Cryst. Liq. Cryst.* **12**, 193 (1971).

³R. Y. Dong and E. Tomchuk, *Phys. Rev. A* **17**, 2062 (1978); K. V. S. Rao, J. S. Hwang, and J. H. Freed, *Phys. Rev. Lett.* **37**, 515 (1976); Y. Poggi, P. Atten, and R. Aleonard, *Phys. Rev. A* **14**, 466 (1976).

⁴Lin Lei and Cai Jundao, "Nematic Liquid Crystals and Landau's Theory of Phase Transitions" (*Scientia Sinica*, Beijing, to be published).

⁵Lin Lei, *Kexue Tongbao* **23**, 715 (1978).

⁶Zhang Zhaoqing, Feng Kean, and Lin Lei, to be published.

⁷M. Suzuki, *Phys. Lett.* **19**, 267 (1965).

⁸T. W. Stinson and J. D. Lister, *Phys. Rev. Lett.* **25**, 503 (1970).

Special Phonons and Superconductivity in the Hexagonal Tungsten Bronzes

W. A. Kamitakahara, K. Scharnberg,^(a) and H. R. Shanks

*Ames Laboratory—United States Department of Energy and Department of Physics,
Iowa State University, Ames, Iowa 50011*

(Received 13 December 1978; revised manuscript received 2 October 1979)

Neutron scattering measurements on single crystals of hexagonal tungsten bronzes $M_{0.33}WO_3$ reveal low-frequency, relatively dispersionless phonon branches which can be associated with the vibrations of the metal atoms M in the large open channels they occupy in the crystal structure. An analysis based on Eliashberg theory shows that the strong dependence of the superconducting transition temperature on the species M arises from these special phonons.

The possibility that the superconducting transition temperature within a group of materials could be raised substantially by varying lattice-dynamical properties has been explored in many studies. However, the direct relation between

changing phonon properties and higher T_c 's, although in principle understood within strong-coupling theory,¹ is difficult to verify experimentally. In this article, experimental results and a suitable analysis are presented showing that, for the

hexagonal tungsten bronzes, substantial changes in T_c are due to a small subgroup of the lattice modes. We regard this as significant, since it reemphasizes the general possibility of optimizing T_c in other systems by varying lattice-dynamical characteristics.

The tungsten bronzes $M_x\text{WO}_3$, where $0 \leq x \leq 1$, exhibit a variety of interesting properties, including unusual superconducting properties. T_c can be several degrees, and for tetragonal Na_xWO_3 , is strongly enhanced² near the phase boundary at $x = 0.2$. For the hexagonal bronzes with $x = 0.33$, T_c shows a considerable variation with the species M , despite the fact that the conduction bands arise from the WO_3 skeleton³ and the electronic structure should be largely independent of M . The structure of the hexagonal bronzes, illustrated by Bevolo *et al.*⁴ and Chesser *et al.*⁵ consists of corner-linked WO_6 octahedra, with the oxygens on the corners shared with adjacent octahedra. Large open channels in the structure are formed by this linkage, into which the M ions can be placed, up to the stoichiometric composition $x = \frac{1}{3}$. The M ions thus tend to be loosely bound. Heat capacity measurements^{4,6} reveal that at low temperatures, $M_{0.33}\text{WO}_3$ compounds have a large excess heat capacity over that of WO_3 itself. By assuming three Einstein oscillators per M atom, with the Einstein frequency dependent on M , Bevolo *et al.*⁴ obtained a very good fit to the excess, thus showing it to arise from vibrations of the M atoms in modes which are fairly well decoupled

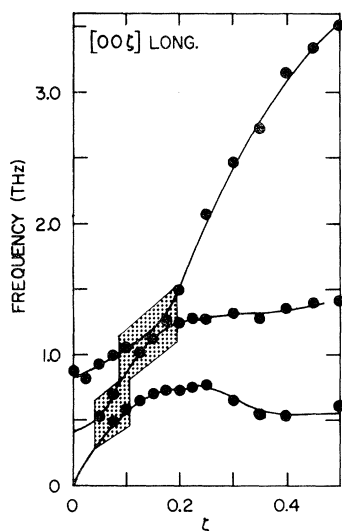


FIG. 1. Low-energy phonon dispersion for $\text{Tl}_{0.33}\text{WO}_3$ longitudinal modes along $[00\zeta]$.

from the WO_3 skeleton. We have observed these modes directly by neutron scattering from single crystals of $\text{Tl}_{0.33}\text{WO}_3$ and $\text{K}_{0.33}\text{WO}_3$, and a powder sample of $\text{Tl}_{0.33}\text{WO}_3$.

The measurements were carried out on triple-axis spectrometers, with use of single-crystal samples grown by a technique described by Shanks.⁷ Powder samples were produced by crushing single crystals. For all specimens, $x = 0.33 \pm 0.01$.

The occurrence of relatively dispersionless modes associated with M atoms is illustrated by the low-energy longitudinal $[00\zeta]$ dispersion curves for $\text{Tl}_{0.33}\text{WO}_3$ shown in Fig. 1. The overall appearance is that of a system in which a normal acoustic phonon branch, which in its unperturbed state rises to 3.5 THz at $\zeta = 0.5$, is hybridized with one almost flat branch at 0.6 THz and another at 1.3 THz. The shaded areas, in which hybridization with the WO_3 skeleton vibrations is occurring, are characterized by broadening of the peaks which we do not understand at present. The dispersion of the WO_3 skeleton vibrations is quite close to the $[00\zeta]$ longitudinal-acoustic-phonon dispersion curve⁸ for cubic Na_xWO_3 . This is to be expected since both cases are determined largely by the energy required to compress or dilate the linked WO_6 octahedra along one of their fourfold axes. The extra modes at 0.6 and 1.3 THz do not appear at all in scans for cubic Na_xWO_3 .

The low-energy $[\zeta\zeta 0]$ transverse modes in $\text{Tl}_{0.33}\text{WO}_3$ (Fig. 2) also give an appearance characteristic of an acoustic branch hybridized with flat branches. In this case, there is definitely one very flat branch at 0.7 THz and possibly another at 1.6 THz.

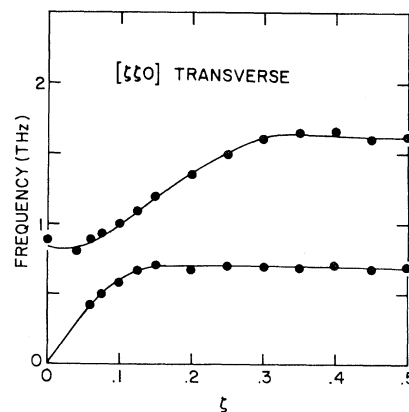


FIG. 2. Low-energy phonon dispersion curves for transverse modes along $[\zeta\zeta 0]$ in $\text{Tl}_{0.33}\text{WO}_3$, polarized perpendicular to the basal plane.

A scan on a powder sample of $Tl_{0.33}WO_3$ (Fig. 3) shows two distinct peaks at 0.6 and 1.4 THz. In contrast, pure WO_3 shows no peaks. The occurrence of two peaks rather than one is reasonable, since the Tl atom sits in a site of hexagonal symmetry. A very good fit to the excess heat capacity⁴ is obtained by assuming two oscillators per Tl atom at 0.6 THz and one at 1.4 THz, showing that the neutron results are completely consistent with the heat-capacity data, and that the partial phonon density of states for the Tl atoms is largely confined to the two peaks.

Measurements of phonon dispersion in $K_{0.33}WO_3$ have been reported previously.⁵ We have taken some supplementary data on $K_{0.33}WO_3$ and find good agreement with the reported results, but our interpretation expands on that of Chesser *et al.*,⁵ who merely noted a large phonon density of states near 1.3 THz, without identifying these states as modes of the K atoms. From our viewpoint, their true nature is made obvious by comparing dispersion curves. The flattened regions near 1.3 THz for $K_{0.33}WO_3$ correspond to similar regions near 0.7 THz for $Tl_{0.33}WO_3$. The K-atom modes are hybridized with the WO_3 vibrations to a greater extent than are the Tl modes. The scattering observed for the Tl modes is more intense than for the K modes because Tl has a larger neutron cross section. The combination of all characteristics, comprising the comparison of dispersion curves (including those⁹ for cubic Na_xWO_3), scattering intensities, powder scans, and heat capacities, makes the identification of the extra branches for the hexagonal bronzes as M -atom modes completely unambiguous.

The most interesting question regarding these special modes is how they affect the superconduct-

ing transition temperature. In all, we have data for T_c (taken as the onset of superconductivity as indicated by heat capacity or susceptibility) on six hexagonal bronzes (Table I). Strong justification exists for expecting that the conduction bands of these compounds depend only slightly on M . Calculations³ for *cubic* $NaWO_3$ show that the conduction bands are almost wholly determined by the WO_3 skeleton, changing very little when the Na is replaced by a vacancy. The Na thus serves only to contribute about one electron per atom to the conduction bands. In fact, the conduction bands of $NaWO_3$, ReO_3 , and $SrTiO_3$ are all rather similar (see Ref. 3 and citations therein), being formed in covalent bonding between oxygen p and transition-metal d orbitals. One expects the conduction bands of hexagonal bronzes to be formed likewise, with little dependence on the species M . The change in T_c should, therefore, reflect the change in the vibrational properties of the M ion. Since the M ions are all chemically similar and reside in virtually identical environments, their mean vibration frequency is primarily determined by their mass, i.e., $\omega_M \sim m^{-1/2}$, where m is the mass of the M ion. On the basis of BCS theory, if superconductivity in these systems were due to the interaction of conduction electrons with these special phonons alone, one would expect a giant isotope effect: $T_c \sim m^{-1/2}$. When the T_c data are plotted versus $m^{-1/2}$ (Fig. 4), the points fall close to a straight line, but the nonzero intercept $T_c \approx 0.7$ K as $m^{-1/2} \rightarrow 0$ is an indication that the vibrational modes of the WO_3 skeleton cannot be neglected.

In our analysis we therefore use an Eliashberg function with two terms,

$$\alpha^2F(\omega) = \frac{1}{2}\omega_M \lambda_M \delta(\omega - \omega_M) + \alpha^2F_{WO_3}(\omega), \quad (1)$$

where the nearly dispersionless special phonons are described by an Einstein spectrum. Note that if $\omega_M \sim m^{-1/2}$, the parameter¹ $\lambda_M = a/m\omega_M^2$, where

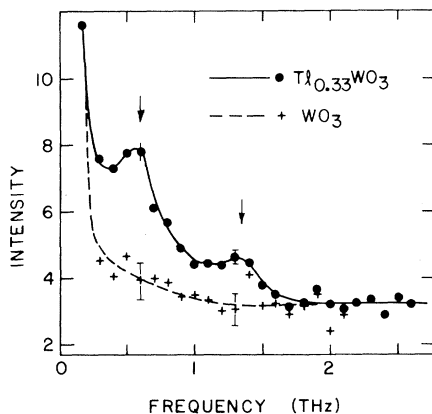


FIG. 3. Scans on bronze powder samples.

TABLE I. Experimental values of T_c and ω_M for $M_{0.33}WO_3$.

M	m (amu)	T_c (K)	ω_M (K)	$m\omega_M^2$ (10^5 amu K ²)
Tl	204.4	1.51	38	2.95
Rb	85.5	1.90	58	2.88
K	39.1	2.34	90	3.17
Cs	132.9	1.12	70	6.51
NH ₄	18.0	3.34
Li	6.9	3.64

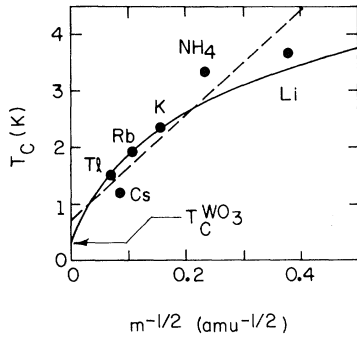


FIG. 4. Dependence of T_c on mass of M ion; the curve was calculated using the Bergmann-Rainer algorithm.

α depends only on electronic structure, should be independent of the species M , and the T_c changes occur at constant λ . In Table I, we show ω_M obtained by combining heat-capacity and neutron data for $M = \text{Rb}, \text{Tl}, \text{K},$ and Cs . Clearly, $m\omega_M^2$ is indeed a constant for Rb, Tl, and K; for Cs, a higher value, perhaps due to the larger ionic radius, is obtained.

Using (1) in the T_c formula of Allen and Dynes⁹ yields

$$T_c = \frac{1}{1.20} \omega_M^{\lambda_M/\lambda} (\omega_{\text{WO}_3}^{\log})^{\lambda_{\text{WO}_3}/\lambda} \times \exp\left(-\frac{1.04(1+\lambda)}{\lambda - \mu^* - 0.62\lambda\mu^*}\right), \quad (2)$$

where $\omega_{\text{WO}_3}^{\log}$ and λ_{WO_3} are averages⁹ over only the second term of Eq. (1), and $\lambda = \lambda_M + \lambda_{\text{WO}_3}$. According to Eq. (2), T_c should vanish for $\omega_M \rightarrow 0$ while λ_M is held constant. Inspection of the general equations¹⁰ for T_c shows this to be incorrect. Consequently, we have calculated the dependence of T_c on $m^{-1/2}$ at constant λ by an exact method, the algorithm of Bergmann and Rainer.¹⁰ (See Fig. 4). In this calculation, the unknown α^2F for the WO_3 skeleton has been approximated by a term $\frac{1}{2}\omega_{\text{WO}_3}\lambda_{\text{WO}_3}\delta(\omega - \omega_{\text{WO}_3})$, and the Coulomb pseudopotential at the cutoff frequency $\omega_N = 10\omega_{\text{WO}_3}$ was chosen to be $\mu^*(N) = 0.1$, which corresponds⁹ to $\mu^* = 0.08$ in Eq. (2). Because $\lambda_M \sim (m\omega_M^2)^{-1}$, we have taken λ_M to be the same for $M = \text{Tl}, \text{Rb},$ and K and $\lambda_{\text{Cs}} = 0.45\lambda_{\text{Tl}}$. With ω_M determined experimentally, we are left with three parameters to fit the T_c 's. For $M = \text{Tl}, \text{Rb},$ and K , one can fit T_c for a wide range of ω_{WO_3} , but to fit T_c^{Cs} a fairly large but physically reasonable value of ω_{WO_3} , about 500 K, is needed. The results are listed in Table II. T_c values obtained from Eq. (2) are

TABLE II. Values for λ_M and λ_{WO_3} (given ω_{WO_3}) which reproduce measured T_c 's for Tl, Rb, and K within 0.02 K; implied values for T_c^{Cs} and $T_c^{\text{WO}_3}$.

ω_{WO_3} (K)	λ_{WO_3}	λ_M	T_c^{Cs}	$T_c^{\text{WO}_3}$
144	0.32	0.22	0.89	0.23
230	0.31	0.19	0.97	0.31
350	0.30	0.16	1.03	0.39

10–20% larger than the exact values, indicating that the Allen-Dynes formula loses accuracy when $\alpha^2F(\omega)$ contains two very different Einstein frequencies. If only one Einstein frequency is present, the formula works very well and we used it to calculate $T_c^{\text{WO}_3}$. The curve in Fig. 4 is calculated for $\omega_{\text{WO}_3} = 230$ K, with λ_M and λ_{WO_3} chosen to fit the T_c values for Rb, Tl, and K (Table II). As one can see, the calculations provide a good description of T_c vs $m^{-1/2}$. The deviations of the data points from the curve (upward for NH_4 , Li, and downward for Cs) are understandable within our interpretation of the role of the special phonons, arising from the influence of ionic size on near-neighbor force constants and thereby on λ_M .

It follows from this analysis that in the hexagonal tungsten bronzes changes associated with a small fraction of the vibrational modes ($\frac{1}{13}$ or less) cause substantial variation in T_c . The qualitative explanation of this dramatic effect involves two factors. The first is the loose binding of the M atoms, which causes λ_M to be fairly large. The second is that we are dealing with rather low- T_c materials, in which the Coulomb repulsion of electrons has been just slightly overbalanced by the electron-phonon interaction due to the WO_3 skeleton. The further increase of the electron-phonon interaction due to the special phonons then causes an increase in T_c which is much larger than the proportionate increase in λ . Our results do not shed light on the enhancement of T_c in tetragonal Na_xWO_3 for x near 0.2, but they do suggest that Na-atom vibrations in the pentagonal channels of the tetragonal bronze structure are important for superconductivity in this phase, thus explaining why the cubic phase ($x > 0.5$), which has no large open channels, is not superconducting.

This work was supported by the U. S. Department of Energy, Contract No. W-7405-ENG-82, Division of Materials Sciences, budget codes AK-01-02-02-1/2. One of us (K.S.) gratefully ack-

nowledges a travel grant from the Deutsche Forschungsgemeinschaft.

^(a)Permanent address: Abteilung für Theoretische Festkörperphysik, Universität Hamburg, Hamburg, West Germany.

¹D. J. Scalapino, in *Superconductivity*, edited by R. D. Parks (Marcel Dekker, New York, 1969).

²H. R. Shanks, *Solid State Commun.* **15**, 753 (1974).

³L. Kopp, B. N. Harmon, and S. H. Liu, *Solid State Commun.* **22**, 677 (1977).

⁴A. J. Bevolo, H. R. Shanks, P. H. Sidles, and G. C.

Danielson, *Phys. Rev. B* **9**, 3220 (1974).

⁵N. J. Chesser, J. G. Traylor, H. R. Shanks, and S. K. Sinha, *Ferroelectrics* **16**, 115 (1977).

⁶C. N. King, J. A. Benda, R. L. Greene, and T. H. Geballe, in *Low Temperature Physics—LT13*, edited by K. D. Timmerhaus, W. J. O'Sullivan, and E. F. Hammel (Plenum, New York, 1974), Vol. 3, p. 411.

⁷H. R. Shanks, *J. Cryst. Growth* **13/14**, 433 (1972).

⁸W. A. Kamitakahara, B. N. Harmon, J. G. Traylor, L. Kopp, H. R. Shanks, and J. Rath, *Phys. Rev. Lett.* **36**, 1393 (1976).

⁹P. B. Allen and R. C. Dynes, *Phys. Rev. B* **12**, 905 (1975).

¹⁰G. Bergmann and D. Rainer, *Z. Phys.* **263**, 59 (1973).

New Evidence for the Two-Electron O⁻ State in GaP

M. Gal,^(a) B. C. Cavenett, and P. Smith

Department of Physics, The University, Hull HU6 7RX, United Kingdom

(Received 6 July 1979)

Optically detected magnetic resonance in oxygen-doped GaP shows that the infrared emission at 0.84 eV and its phonon replicas are due to a spin-triplet to -singlet transition of the two-electron state of oxygen. The resonance data also show that the two-electron center has axial symmetry along the [110] axis, indicating that after capturing the second electron a strong lattice relaxation takes place.

The role of oxygen in GaP has been studied extensively for many years by various techniques,¹ but the nature of the two-electron oxygen-related electronic states is still a matter of controversy. Experiments have shown that oxygen is a deep donor on a P site and that the neutral donor binds an electron by 0.895 eV at 1.6 K. Dean and Henry² have shown that in addition to the donor-acceptor transitions involving the deep oxygen donor, another infrared luminescence emission is also due to oxygen. A zero-phonon line at 0.84 eV accompanied by phonon replicas has been shown to shift upon replacing ¹⁶O by ¹⁸O. The luminescence was thought to result from a radiative transition of an electron from the excited 1s *E* state of the isolated oxygen donor to the 1s *A* ground state. In 1973, by using photocapacitance measurements, Kukimoto, Henry, and Merritt³ and Henry⁴ discovered that the deep O donor in GaP could bind two electrons to become O⁻. After binding the first electron, the donor could capture a second electron with a subsequent large lattice displacement indicating that a substantial change in the O⁻ host bonds had taken place. Grimmeiss *et al.*⁵ and Morgan,⁶ on the other hand, interpreted their two-electron photocapacitance data by supposing that the selection rules were

such that optical transitions between the *X*₁ conduction-band edge and the two-electron ground state were very weak and this could explain the observed high optical threshold energies without involving a large Franck-Condon shift. Recently, Morgan⁷ reinterpreted the infrared spectra of Dean and Henry,² suggesting that the 0.8-eV emission involved radiative transitions of the second electron bound to oxygen. His conclusions were based on the differences between the phonon modes involved in the infrared spectra and those involved in the neutral-oxygen donor-to-acceptor pair luminescence.

We have studied the electron states in oxygen-doped GaP by the optically detected paramagnetic resonance (ODMR) technique. Our results show that the emitting level of the 0.84-eV transition, observed first by Dean and Henry,² is a spin triplet. The orientation dependence of the ODMR spectra and the observed strong hyperfine interaction with *one* Ga nucleus show that the symmetry of the center is lower than tetrahedral. These results can be explained if we suppose that the infrared band is a triplet-to-singlet transition of the two-electron O⁻ state, in agreement with Morgan,⁷ and that after capturing the second electron lattice relaxation oc-